Graphical design of world map projections

Bernhard Jenny[a]; Tom Patterson[b]; Lorenz Hurni[a]

[a] Institute of Cartography, ETH Zurich, Zurich, Switzerland [b] US National Park Service, Harpers Ferry, WV, USA

First published on: 28 September 2010

PLEASE SCROLL DOWN FOR ARTICLE

Taylor & Francis
Taylor & Francis Group

Graphical design of world map projections

Bernhard Jenny[a]*, Tom Patterson[b] and Lorenz Hurni[a]

[a]Institute of Cartography, ETH Zurich, Zurich, Switzerland; [b]US National Park Service, Harpers Ferry, WV, USA

The design of new map projections has up until now required mathematical and carto-graphic expertise that has limited this activity to a small group of specialists. This article introduces the background mathematics for a software-based method that enables carto-graphers to easily design new small-scale world map projections. The software is usable even by those without mathematical expertise. A new projection is designed interactively in an iterative process that allows the designer to graphically and numerically assess the graticule, the representation of the continents, and the distortion properties of the new projection. The method has been implemented in Flex Projector, a free and open-source application enabling users to quickly create new map projections and modify existing projections. We also introduce new tools that help evaluate the distortion properties of projections, namely a configurable acceptance index to assess areal and angular distor-tion, a derived acceptance visualization, and interactive profiles through the distortion space of a projection. To illustrate the proposed method, a new projection, the Cropped Ginzburg VIII projection, is presented.

Keywords: small-scale map projections; acceptance index; Flex Projector; Cropped Ginzburg VIII projection

1. Introduction

The design of new map projections has hitherto required mathematical and cartographic expertise and has therefore been reserved to a small group of specialists. The method proposed in this article is based on a user-friendly software application called Flex Projector that strives to simplify and to democratize the making of world map projections so that more cartographers will be able to design such projections. Flex Projector lets the author of a projection visually design the graticule and provides specialized tools for distortion analysis, resulting in a new graphical approach to the design of world map projections.

World map projections are typically intermediate projections that are neither conformal nor equal-area. While the equal-area property of projections has long been regarded as the most important property for world maps, projections with intermediate distortion character-istics have become increasingly popular for world maps, mainly because they better preserve the shape of continents (Canters 2002, p. 57).

In the following paragraphs, we focus on the mathematics behind the graphical user interface of Flex Projector and introduce new tools for assessing projections. After giving an overview of customization approaches of small-scale map projections, we introduce the

equations of our method that translate user-definable settings into a new projection. To visualize and assess the distortion pattern of a projection, the following four new interactive tools are available: (1) a customizable acceptance index integrating areal and angular distortion; (2) a related acceptance visualization; (3) interactive cross-sections for generating distortion profiles; and (4) diagrams of the adjustment curves with their derivatives, specific to our method. These four tools complement the graphical approach to projection design by providing numerical and graphical indications about the distortion properties of a new projection. Finally, the Cropped Ginzburg VIII projection, a new pseudocylindrical projection for world maps, is introduced, which was designed with the described method.

2.   Previous approaches to customized small-scale projections

Classical small-scale map projections are defined by a pair of transformation formulae that are derived either by a rigorous mathematical development or by trial-and-error, i.e. the projection formulae are recursively adjusted until certain geometry or distortion requirements are satisfied. Alternative systematic approaches for the customization of map projections have been developed. Canters (2002) identifies two groups relevant to this discussion.

- The equations of a parent projection can be generalized to allow independent adjustments of certain graticule characteristics (e.g. the length of the pole line or the ratio of the axes). This approach has been pioneered by Wagner and Siemon and has resulted in the Wagner projection family (see Canters 2002, p. 119 for references). Another example is the family of hyperelliptical pseudocylindrical projections by Tobler (1973). As Canters (2002) notes, with this approach, the nature of the modified projection is strongly determined by the graticule of the parent projection.
- This family of projections expresses the relation between map projection coordinates and geographical longitude and latitude by means of power series. Urmayev pioneered this approach for pseudocylindrical projections (Bugayevskiy and Snyder 1995, p. 55). Ginzburg proposed five polyconic projections based on polynomials (Snyder 1993, p. 248–250, Bugayevskiy and Snyder 1995, p. 143–149). Snyder (1985), Canters (1989, 2002), and Laskowski (1991) presented other pseudocylindrical and polyconic projections based on polynomials.

These two groups of techniques are appropriate for pseudocylindrical and polyconic projections, which can be used for small-scale maps. We deliberately limit this discussion to such projections and ignore azimuthal, cylindrical, and conical projections, as these are not generally recommended for small-scale world maps (Snyder 1987, p. 34, Slocum *et al.* 2009).

Systematic approaches to map projection design require evaluation criteria to assess the quality of a projection. Using measures for local distortion characteristics, so-called minimum-error projections can be developed, generally in combination with the least-squares or the simplex method for the minimization of projection distortion (see Tobler 1977 for examples, see Canters 2002 for an overview). The approaches outlined above take into account geometrical constraints that govern the shape of the resulting graticule. However, controlling the graphical appearance of automated low-error methods is generally not trivial and not appropriate for visually designing map projections.

A complementary visual approach for the definition of map projections was pioneered by Arthur Robinson (Robinson 1974). Robinson graphically developed a pseudocylindrical

projection defined by two tables, with one table specifying the length of parallels and the other table giving the distance of parallels from the equator. Hence, Robinson does not provide a pair of equations for transforming the spherical longitude λ and latitude φ to projected *X/Y* map coordinates. The mapping is instead defined for discrete points on a five-degree grid. A similar approach was also taken by Baranyi (1968) for defining a series of intermediate pseudocylindrical projections.

3.   Extending and customizing Robinson's projection

Robinson's projection is defined by two tables. The first table describes the length of parallels for every five degrees of increasing latitude. The second table of parameters defines the distance of each parallel from the equator, also in steps of five degrees of increasing latitude (Figure 1). The quadrant shown in Figure 1 is mirrored along the horizontal and the vertical axis to construct the full graticule. Robinson proceeded through an iterative process to create his pseudocylindrical projection, graphically evaluating the appearance and relative relationships of landmasses, until he estimated that further adjustments would produce no improvement (Robinson 1974, p. 151–152). Robinson's projection was very well received by cartographers and widely used, for example by the National Geographic Society (Garver 1988).

Robinson's tabular parameters have to be interpolated for longitude/latitude pairs that do not align with the five-degree grid. Indeed, Robinson (1974) did not stipulate which interpolation to use, which leads to incompatible implementations of his projection, as various methods have been used, each resulting in a slightly different projection. For example, Snyder (1990) applies the central-difference formula by Stirling, which the United States Geological Survey (USGS) adopted for GCTP.[1] Cubic spline interpolation is used by Ratner (1991) for Intergraph software and by Evenden (2005) for the PROJ.4 library, which is widely used by various open-source Geographic Information Systems (GIS).[2] It was not until 1989 that Richardson (1989) reported that Robinson used the Aitken interpolation procedure.

Interpolation of the tabular parameters can be avoided when analytical expressions are developed that take longitude and latitude as input parameters and output *X/Y* coordinates on the map (Canters and Decleir 1989, Beineke 1991). Such classical projection formulae can be simpler to implement and are possibly faster to compute, as no interpolation is required.

The method proposed in this article is based on Robinson's graphical approach to map projection design. It treats the graticule as a flexible grid that the designer of a projection can
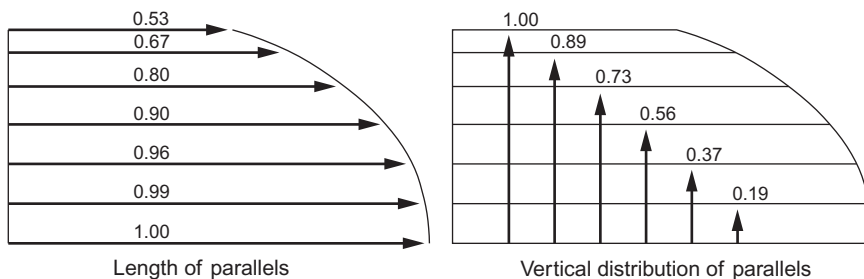

Figure 1.   The two sets of tabular parameters of the Robinson projection. Note: Only a third of the parameter values are shown.

adjust in shape and size. Robinson's approach is extended with the option to bend parallels and to adjust the distance between meridians. Adjustments to the graticule are controlled by four tables defining (1) the horizontal length of parallels, (2) the vertical distance of parallels from the equator, (3) the distribution of meridians, and (4) the bending of parallels. Additionally, the height-to-width ratio of the graticule can be chosen, as well as the internal scale factor and the slope of meridians at the poles and the equator.

The goal of this graphical method, which emphasizes the shape of continents and the form of the resulting map graticule, is to make the design of world map projections approachable for those without expert knowledge in mathematics. Figure 2 shows a screenshot of the graphical interface of Flex Projector with sliders to adjust the length of parallels for every five degrees. Jenny and Patterson (2007) and Jenny *et al.* (2008) provide an overview of the functionality and interface of this cross-platform and open-source application from a user's point of view. This section explains how the user-defined tabular parameters are used to transform geographical coordinates into *X/Y* coordinates on the map. The formulae presented here assume that the discrete tabular data are converted to continuous curves and are based on a spherical earth model. The necessary interpolations for the four curves are discussed at the end of this section.

3.1.   *Length and distribution of parallels*

Equation (1) is Robinson's projection, with one formula defining the length of parallels and another formula defining the distance of parallels from the equator (Robinson 1974). Parameter l_φ, determines the length of the parallel at latitude φ and d_φ determines the distance of the parallel from the equator (Figure 1). l_φ and d_φ are continuous curves derived from tabular data. Equation (1) computes x by scaling the longitude λ with l_φ and y by multiplying d_φ with k, which is a constant factor that specifies the height-to-width ratio of the projection. R is the radius of the generating globe at the scale of the map as drawn, which determines the *nominal* scale of the resulting map (the actual size of the graticule) and is chosen by the mapmaker. The *internal* scale factor s defines the relationship between the size of the graticule and the size of the generating globe and is chosen by the projection designer.

$$
\begin{aligned}
x &= Rsl_\varphi\lambda \quad l_\varphi[0\ldots1] \\
y &= Rskd_\varphi\pi \quad d_\varphi[0\ldots1]
\end{aligned}
\tag{1}
$$

The internal scale factor s is not unique to Robinson's projection, as many pseudocylindrical projections use similar factors [e.g. various projections by Eckert, Putniņš, and Wagner (see for example Fenna 2007 for equations)]. Robinson chose s in Equation (1) such that the surface of the projected graticule equals the area of the generating globe with radius R.

An alternative is to choose s such that it minimizes areal distortion of the projection. This is achieved by finding the minimum of the weighted mean error in areal distortion D (Equation 2), m is the number of points in a regular grid based on an equal spacing of longitude and latitude values covering the sphere, a_j and b_j are the principal scale factors (half the length of the major and minor axis of Tissot's indicatrix) for the grid cell j, and p is 1 if $a_j b_j \geq 1$ and -1 otherwise (Canters and Decleir 1989). a_j and b_j are computed from partial derivations of x and y with respect to φ and λ (Canters and Decleir 1989, p. 13). Areal distortion is weighted by the cosine of the latitude to take into account the decrease in area for grid cells when moving from the equator to the pole.
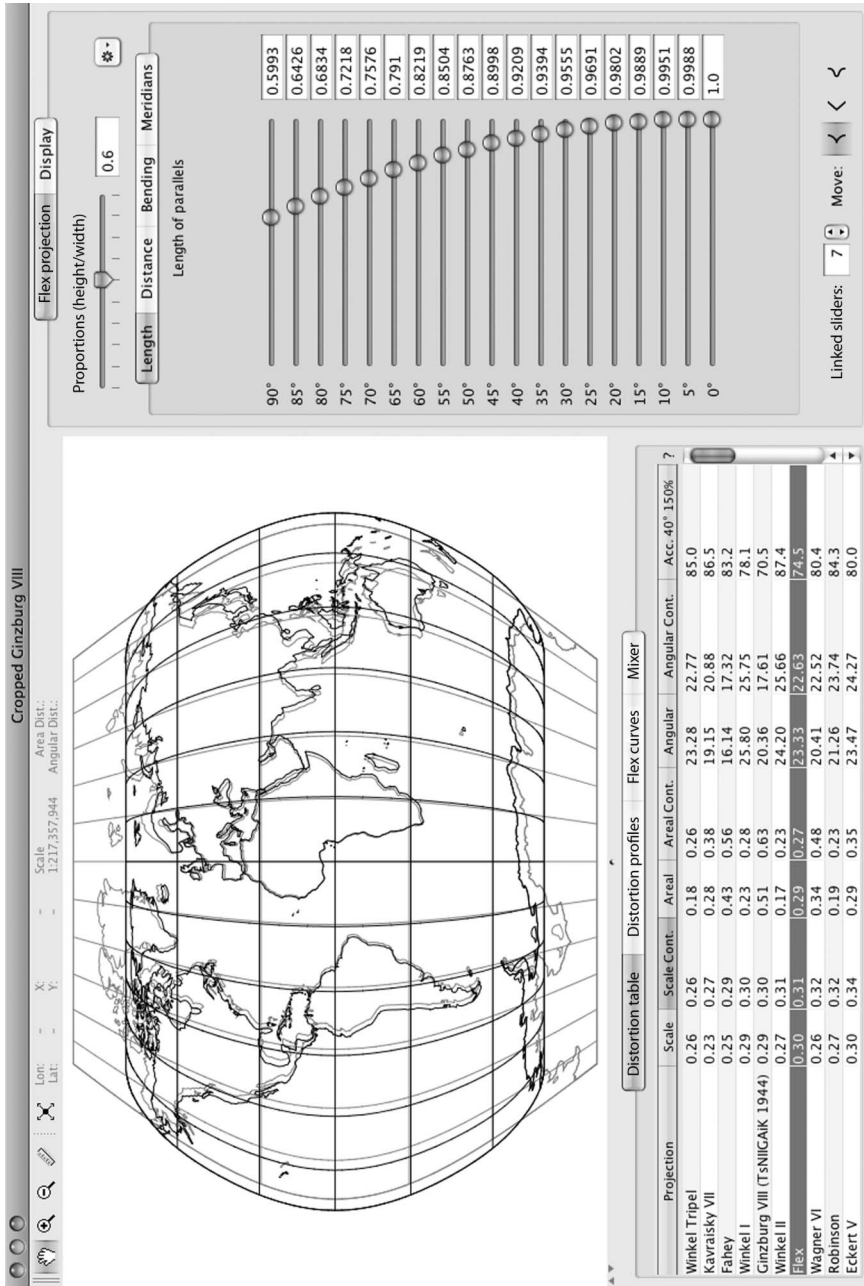
Figure 2. Screenshot of the Flex Projector. Black: the Cropped Ginzburg VIII projection. Grey: the original Ginzburg VIII projection. Right panel: sliders for adjusting the length of parallels. Bottom left panel: ordered distortion indices.

$$D = \frac{1}{S}\sum_{j=1}^{m}\left[(a_j b_j)^p - 1\right]\cos\varphi_j \quad \text{with } S = \sum_{j=1}^{m}\cos\varphi_j \qquad (2)$$

3.2. Distribution of meridians

With Robinson's projection, meridians are equally spaced along the parallels, which results in a *true* pseudocylindrical projection (Snyder 1993, p. 189). Equation (3) extends the computation of x of Equation (1) with the displacement factor m_λ, which is a continuous curve derived from tabular data, varying with longitude λ. d_m is the distance between two values in the table (for example 15°) and $\text{sgn}(\lambda)$ is −1 for negative longitudes and +1 for positive longitudes. Figure 3 illustrates how the distribution of meridians can be adjusted. Values for m_λ smaller than 0 displace the meridian towards the central meridian and values for m_λ larger than 0 move the meridian in the opposite direction.

$$x = Rsl_\varphi(\lambda + \text{sgn}(\lambda)m_\lambda d_m) \qquad (3)$$

3.3. Bending of parallels

Pseudocylindrical projections portray parallels as straight lines. Our method was extended to include polyconic projections, i.e. projections with bended parallels that form non-concentric circular arcs. The designer of a projection defines the amount of bending f_φ for a parallel at latitude φ (Figure 4). Negative values of f_φ are transformed to concave bending and positive values to convex bending relative to a horizontal reference line. Equation (4) converts f_φ to the bending factor $f_{\lambda\varphi}$, which is the amount of bending at longitude λ and latitude φ. Equation (4) also generalizes the formula for the y coordinate (Equation 1) by including the bending factor $f_{\lambda\varphi}$.

Parallels are moved towards the equator, but not towards the poles to ensure that arced parallels remain within the bounding box imposed by the user-definable height-to-width ratio k. If the amount of bending f_φ is smaller than 0, concave bending is applied and the displacement is maximum at the central meridian (where λ equals 0 and $f_{\lambda\varphi}$ equals $1 + f_\varphi$). The displacement diminishes to zero at the end of the parallel (where λ equals π and
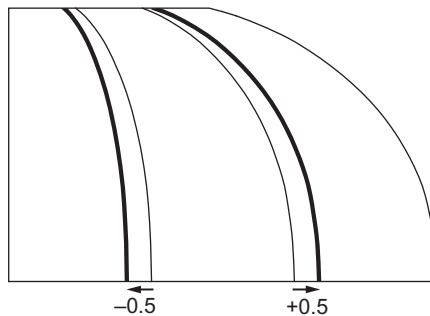

Figure 3.   Impact of the displacement factor m_λ on the distribution of meridians.
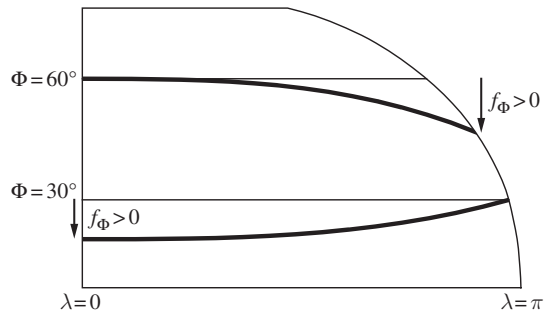
Figure 4. User-definable bending of parallels. Note: Only parallels at 30° and 60° latitude are shown.

$f_{\lambda\varphi}$ equals 1, see the parallel at 30° latitude in Figure 4). If f_φ is larger than 0, convex bending is applied in an analogous manner, but with a maximum displacement at the end of the parallel and no displacement at the central meridian (see the parallel at 60° latitude in Figure 4).

$$y = Rskd_\varphi f_{\lambda\varphi}\pi$$
$$f_{\lambda\varphi} = 1 + f_\varphi\left(1 - \frac{\lambda^2}{\pi^2}\right) \quad \text{for } f_\varphi < 0 \text{ (concave bending)}$$
$$f_{\lambda\varphi} = 1 - f_\varphi\left(\frac{\lambda^2}{\pi^2}\right) \qquad \text{for } f_\varphi > 0 \text{ (convex bending)}$$

(4)

Equation (4) uses a quadratic decrease, i.e. arcing diminishes with the square of longitude λ. Other types of decreasing functions, such as cubic or sine curves, generate parallels with slightly different arcing and can be derived similar to Equation (4).

3.4. *Cubic spline interpolation*

The method presented here uses cubic splines for the interpolation of continuous curves through the user-defined control points. Cubic splines offer the following advantages for cartographic projections (Ratner 1991): (1) they are twice continuously differentiable, resulting in smooth curves; (2) the evaluation of cubic splines is very quick; (3) derivatives can be efficiently computed; (4) and inverse formulae may be realized. Cubic spline interpolation is a piecewise interpolation, i.e. a cubic curve is computed for each piece between two consecutive points. Boundary conditions must be introduced to define the two ends of the curve. For the Robinson projection, Ratner (1991) specifies the first derivatives at the end of the curves, whereas Beineke (1991) uses a combination of first and second derivatives.

With our method, three curves use the so-called natural boundary condition, which implies a vanishing second derivative at both ends of the curve. They are: (1) the curve adjusting the distance of parallels from the equator, (2) the curve for bending the parallels, and (3) the curve that adjusts the distribution of meridians. The distance and the bending
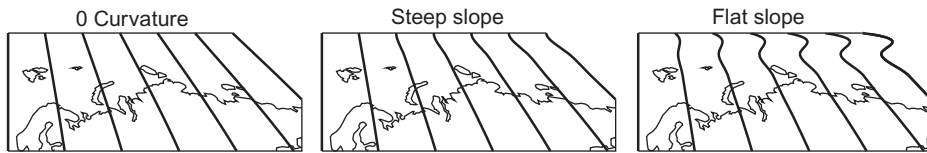
Figure 5. Boundary conditions at poles. Note: Extreme slope values are used for illustration purposes.

curves have user-definable support points every five degrees. The curve for the distribution of meridians has support points every 15 degrees.

For the curve defining the length of parallels, the boundary conditions at the poles and at the equator can be chosen. At the poles, the curvature can be set to 0, which results in meridians abutting the pole line as straight lines. Alternatively, a slope value can be imposed for curved meridians as well (Figure 5).

4. Evaluating projection distortion

The design of a new projection is an iterative process that requires many trial adjustments and continuous assessment of the resulting distortion properties. To support the designer of a new projection, specialized tools are therefore needed to quickly and easily assess each adjustment.

The visual appearance of the graticule and the continental coastlines should be the primary factor when assessing the appropriateness of a new projection. This admittedly subjective approach to the design or selection of a map projection must be complemented by a careful evaluation of the distortion properties. Specialized tools are needed, either numerical indices or graphical devices.

Numerical indices generally summarize the distortion for the whole graticule. Three useful indices are (1) the weighted mean error for areal distortion (Equation 2); (2) the weighted mean error for overall scale distortion; and (3) the mean angular distortion index (Canters and Decleir 1989, Canters 2002). Of these three, only the weighted mean error for overall scale distortion integrates areal and angular distortion. Other indices have been proposed, but, as Canters and Decleir (1989) point out, none of them satisfactorily integrates areal and angular distortion. An interesting addition is Čapek's Q index, which summarizes overall projection distortion (Čapek 2001, see discussion below).

While numerical indices are useful tools to detect high distortion values at a global level, it must be stressed that they should be interpreted with caution, as the ranking of projections will depend on the index chosen (Canters 2002).

Various graphical devices exist that can help the user visualize the local variability of distortion patterns. Examples include Tissot's classic indicatrices, which illustrate local area and angular distortion, and isolines of angular and areal distortion showing distortion patterns in a spatially continuous way (Figure 6). They are computed from local area scale σ_j (Equation 5) and the maximum angular distortion ω_j (Equation 6). Isolines are commonly used today (e.g. Canters and Decleir 1989) and are an excellent source for detecting locally strong variations in the distortion pattern that would otherwise remain invisible.
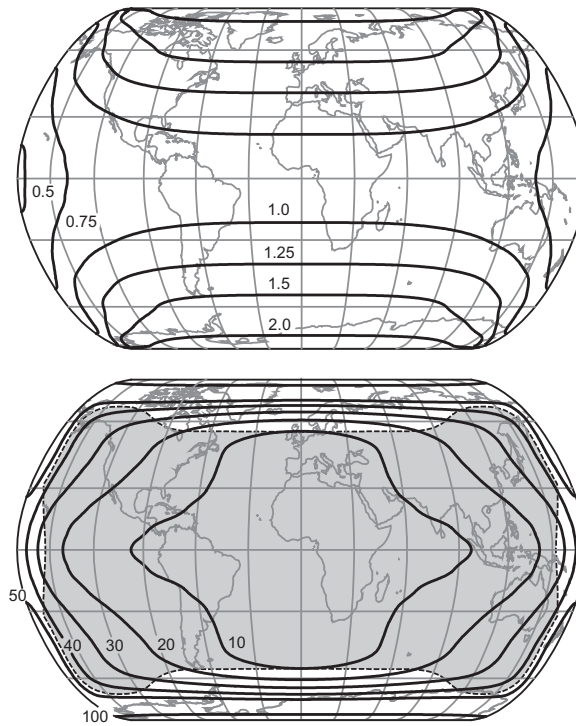
Figure 6. Isolines of areal (top) and angular (bottom) distortion for the Cropped Ginzburg VIII projection. The bottom figure shows the area in grey with ω_{acc} smaller than 45° and σ_{acc} smaller than 150% (see Section 4.2.).

$$\sigma_j = a_j b_j \tag{5}$$

with a_j and b_j being the scale factors along the principal directions at position j on the sphere.

$$\omega_j = 2 \arcsin \frac{a_j - b_j}{a_j + b_j} \tag{6}$$

4.1. Acceptance index

The Q index by Richard Čapek summarizes overall projection distortion integrating areal and angular distortion (Čapek 2001). Čapek builds on the idea that for any given map, areal and angular distortion can only be accepted up to a certain level. For every other degree on a sphere, he computes the area scale σ_j (Equation 5), which expresses the local area inflation or deflation, and the maximum angular distortion ω_j (Equation 6), corresponding to the local maximum angular distortion. This results in two grids covering the sphere, with the cells containing measures for areal and angular distortion. He then compares for each cell the angular distortion with 40° and the area scale with 150% of a reference area. The distortion thresholds that Čapek considers to be acceptable are 40° and 150%. He then sums the grid cells with distortion values below the thresholds,

weighted by the cosine of the latitude to take into account the decrease in area when moving from the equator to the pole (Equation 7). To determine whether an areal inflation or deflation value is acceptable, Čapek uses the smallest area scale σ_{min} in the grid as a reference.

$$Q = \frac{\sum_{j=1}^{m} P_j \cos \varphi_j}{\sum_{j=1}^{m} \cos \varphi_j} \tag{7}$$

with $P_j = 1$ if $\sigma_j < 1.5\sigma_{min}$ and $\omega_j < 40°$; otherwise $P_j = 0$

The Q index as defined by Čapek is sensitive to the magnitude of extreme compression in the graticule. Because the Q index quantifies areal distortion in each part of the projection by comparing local area variation to the smallest area scale σ_{min} that occurs in the graticule, the calculation of areal distortion will strongly depend on extreme compression values. As such, projections will score a low Q value if they are characterized by a strong compression of small parts of the graticule, even if overall the distortion of area in the projection is moderate. Our modified index, called acceptance index A, deviates from Čapek's Q index by using a reference value σ_{min} of 1 for accepting or rejecting areal distortion. It also differs from the original Q index in that the user can choose the threshold values ω_{acc} and σ_{acc} for acceptable angular and areal distortion, leading to Equation (8).

$$A = \frac{\sum_{j=1}^{m} P_j \cos \varphi}{\sum_{j=1}^{m} \cos \varphi_j} \text{ with } P_j = 1 \text{ if } \sigma_j \in \left[\frac{1}{\sigma_{acc}}; \sigma_{acc}\right] \text{ and } \omega_j < \omega_{acc}; \text{ otherwise } P_j = 0 \tag{8}$$

The acceptance index A gives equal weight to an areal stretching by σ_{acc} and an areal compression by $1/\sigma_{acc}$. For example with σ_{acc} equal to 2, inflation up to 200% and compression down to 50% are accepted. The same logic is used by Canters and Decleir in Equation (2) for calculating overall areal distortion. Hence, the surface patches are summed if for the patch j two conditions are met: (1) the area scale σ_j is larger than $1/\sigma_{acc}$ and smaller than σ_{acc}; and (2) the maximum angular distortion ω_j is smaller than the acceptable angular distortion ω_{acc}. The final acceptance A is the sum of all patches satisfying these conditions, weighted by the cosine of the latitude.

Čapek's Q index and our acceptance index A are complementary. When evaluating distortion on world map projections, it is usually the shape of the continents and the relative variation of area that is most important, as world maps are seldom used to perform area measurements. Rather, they are used to visualize spatial data at the global scale. Čapek's Q index is based on this idea and measures relative area variation by normalizing against the minimal local areal distortion.

The acceptance index A is normalized against an undistorted reference area and is therefore useful when area measurements need to be made on the map. In the context of designing new projections, the acceptance index A reflects changes to the *internal* scale factor s (Equations 3 and 4), which enlarges or reduces the graticule without changing its

shape. (Note that the *internal* scale factor *s* is independent of the *nominal* scale for displaying the map.) The designer of a projection can set *s* to an arbitrary value. Depending on the purpose of the map, one of the following three values may be preferred: (1) *s* set to minimize overall areal distortion as expressed by Equation (2) for maps that support approximate area measurements; (2) *s* set to generate a graticule with the area of the generating sphere, as Robinson did for his projection; or (3) *s* set to remove areal distortion at a selected point when measurements are expected to be made around a point of interest. Flex Projector, the tool for designing new projections, lets the user select one of the three criteria and automatically adjusts *s* during the design process.

4.2. Acceptance visualization

Similar to isolines of distortion, an acceptance visualization can be generated from local acceptance values. Figure 6 (bottom) shows acceptable areas for the Cropped Ginzburg VIII projection (which will be introduced below) with a darker shade. For the example in Figure 6, the authors chose a threshold for the maximum angular distortion of 45° and a threshold for the area scale of 150%. The darker shade indicates where areal and angular distortion as defined by Equations (5) and (6) are below the thresholds. A cell is shaded when P_j as defined in Equation (8) is 1.

It is hoped that the acceptance index and the acceptance visualization are easy to understand for designers of new projections. The user can observe in real time how the *A* index and the acceptance visualization change when the thresholds for acceptable angular and areal distortion are adjusted to the purpose of the map and the data mapped. Hence, the acceptance index and the acceptance visualization are not static, but interactive user-definable tools to explore the distortion characteristics of a projection.

4.3. Distortion profiles

Horizontal and vertical distortion profiles are other ways to visualize and interactively explore the distortion characteristics of a projection. They are updated in real time while the user adjusts the position of the profiles with two sliders. Figure 7 shows a section of the user interface in Flex Projector with distortion profiles along the central meridian and at a latitude of $\pm 60°$. The profiles show the area scale and the maximum angular distortion (Equations 5 and 6) along a horizontal and a vertical cut. The bold lines on the map indicate the location of the profiles and move when the sliders change.

4.4. Derivatives of curves

Distortion profiles are useful for detecting locally strong variations in the distortion characteristics of a projection. But when designing a new projection with Flex Projector, it can be difficult to identify the exact reason for the discontinuities just by looking at the profiles. A closer examination of the individual curves can often help identify the reasons. Especially, the first derivatives of the curves can indicate which support point in the curve needs to be adjusted to eliminate the discontinuity. Flex Projector displays and updates the curves and their derivatives in real time as shown in Figure 8.
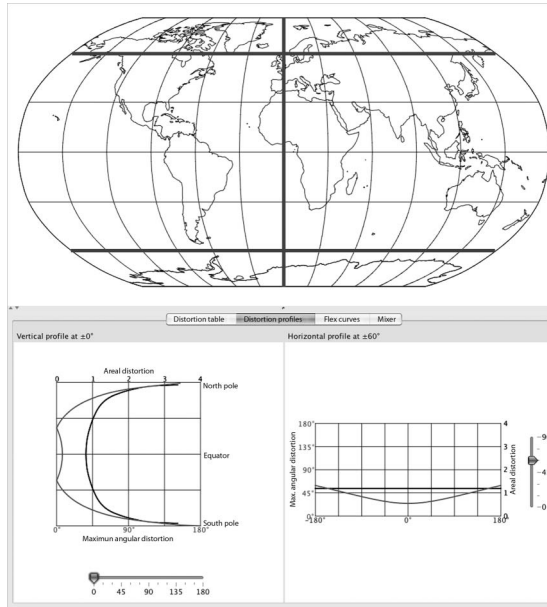
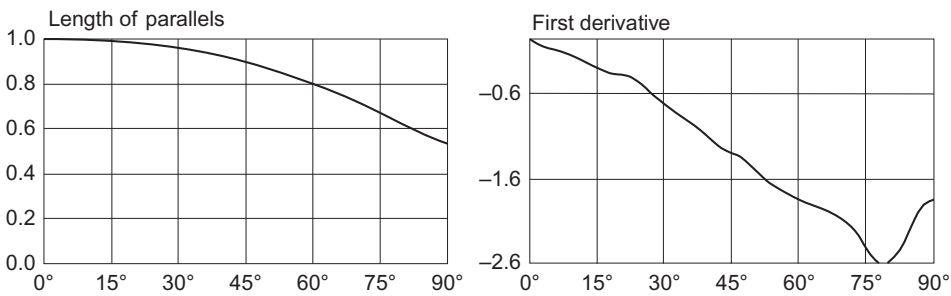Figure 7.   Distortion profiles for the Robinson projection.

Figure 8.   Curve for the length of parallels for the Robinson projection and its derivative.

5.   Creating the Cropped Ginzburg VIII projection

G.A. Ginzburg was a cartographer working at the Russian TsNIIGAiK institute (Ginzburg 1949, referenced by Maling 1960, Snyder 1993). In 1944, he introduced his pseudocylind-rical Ginzburg VIII projection (Figure 9), which is therefore also known as 'TsNIIGAiK 1944'. It was developed to improve the representation of the Soviet Union on world maps with the central meridian at 70° east. Meridians are not equally spaced, but are closer near the border of the graticule. It is an intermediate projection, i.e. neither conformal nor equal-area. The projection prominently portrays continental shapes in a relatively large central area of the graticule. Despite this advantage, the Ginzburg VIII projection has not been used widely, probably because of its strong inflation of polar regions. Indeed, its distribution of parallels is unusual for intermediate projections, as the spacing between parallels increases towards the poles (Canters 2002, p. 35).
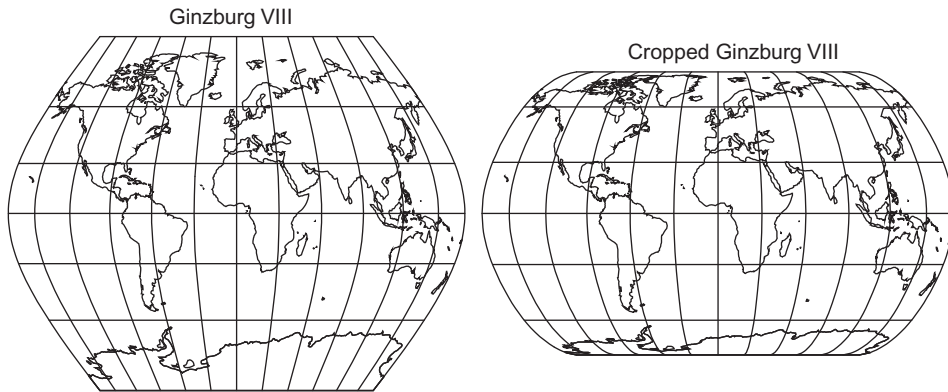
Figure 9. The Ginzburg VIII and the Cropped Ginzburg VIII projections.

An improvement to this projection, called Cropped Ginzburg VIII, is therefore proposed here, which compresses extreme latitudes in the N–S direction and thereby reduces the height-to-width ratio of the projection from 0.78 to 0.6. Reducing the proportions not only diminishes area inflation in the polar regions, but also reduces the projection height (Figure 9). The Cropped Ginzburg VIII projection retains the irregular distribution of meridians. As with the original Ginzburg VIII projection, the distance between parallels increases with growing latitude up to 50° north, but decreases above this limit. The projection also differs from many other projections by its smooth corners where the horizontal polar line and the bounding meridian lines meet. The Cropped Ginzburg VIII projection has a compact form that shows the continents in the central area without much shape distortion up to relatively high latitudes, as illustrated by the isolines of areal and angular distortion in Figure 6. Table 1 compares the distortion characteristics of the Cropped Ginzburg VIII projection with other popular projections, showing that the amount of distortion is within acceptable limits. See Table 2 for the projection parameters.

Table 1. Distortion indices for the Cropped Ginzburg VIII projection and other world map projections (smaller values are better, except for the acceptance index). Indices after Canters and Decleir (1989).

	Weighted mean error for overall scale distortion	Weighted mean error for areal distortion	Mean angular distortion index	Acceptance index A σ_{acc} =150%; ω_{acc} = 40°
Kavraisky VII	0.23	0.28	19.15	86.5
Winkel Tripel	0.26	0.18	23.28	85.0
Robinson	0.27	0.19	21.26	84.3
Cropped Ginzburg VIII	0.29	0.29	23.34	80.9
Eckert IV	0.36	0	28.73	81.9
Miller cylindrical	0.39	1.30	7.63	62.9
Mollweide	0.39	0	32.28	70.6

Table 2. Parameters for the Cropped Ginzburg VIII projection.

φ	Parallels length l_φ	Parallels distance d_φ	λ	Meridian distribution m_λ
0	1	0	0	0
5	0.9988	0.0590	15	0.11935
10	0.9951	0.1183	30	0.23855
15	0.9889	0.1778	45	0.3567
20	0.9802	0.2382	60	0.47155
25	0.9691	0.2994	75	0.57885
30	0.9555	0.3618	90	0.67145
35	0.9394	0.4254	105	0.7388
40	0.9209	0.4906	120	0.7663
45	0.8998	0.5570	135	0.7344
50	0.8763	0.6241	150	0.618
55	0.8504	0.6901	165	0.38595
60	0.8219	0.7540	180	0
65	0.7910	0.8130		
70	0.7576	0.8665		
75	0.7218	0.9140		
80	0.6834	0.9550		
85	0.6426	0.9843		
90	0.5993	1		
Height/width k		0.6		
Scale s		0.803		

6. Conclusion

The indisputably best projection for world maps does not exist. Because maps depict different types of data and have different visualization goals, cartographers use a variety of projections that exhibit unique properties. Even when a map has a clearly defined goal, cartographers will still disagree on the choice of the projection. Our method should facilitate the development and design of custom projections, based on rational criteria. The tools presented in this article for the assessment of distortion characteristics help in the objective evaluation and selection of world map projections. In combination with Tissot's indicatrices and isolines of angular and areal distortion, a compromise between the graphical appearance of a graticule and its distortion characteristics can be achieved. The tools presented in this article might even make cartographers rethink their habitual choice of projections and maybe develop improved new projections.

The Cropped Ginzburg VIII projection is but one example of a multitude of new projections that users of Flex Projector will hopefully create in the future. Jenny *et al.* (2008) provide some guidelines and practical tips for the creation of new projections with the method presented here and also describe the design of two new projections (the Natural Earth and the A4 projections) that could inspire interested readers to create their own projection.

Acknowledgements

Notes

1. GCTP (General Cartographic Transformation Package) is an open-source projection library available for free from http://edcftp.cr.usgs.gov/pub//software/gctpc/
2. The development of PROJ.4 started in the early 1980s at the USGS with much of the code derived from GCTP. It is available from http://www.remotesensing.org/proj/. An enhanced version called libproj4 is available from http://members.verizon.net/~vze2hc4d/proj4/

References

Baranyi, J., 1968. The problems of the representation of the globe on a plane with special reference to the preservation of the forms of continents. *In*: *Hungarian cartographic studies*. Budapest: Földmérési Intézet, 19–43.

Beineke, D., 1991. Untersuchung zur Robinson-Abbildung und Vorschlag einer analytischen Abbildungsvorschrift. *Kartographische Nachrichten*, 41, 85–94.

Bugayevskiy, L.M. and Snyder, J.P., 1995. *Map projections: a reference manual*. London: Taylor & Francis.

Canters, F., 1989. New projections for world maps, a quantitative-perceptive approach. *Cartographica*, 26, 53–71.

Canters, F., 2002. *Small-scale map projection design*. London: Taylor & Francis.

Canters, F. and Decleir, H., 1989. *The world in perspective: a directory of world map projections*. Chichester: John Wiley and Sons.

Čapek, R., 2001. Which is the best projection for the world map? *In*: *20th International Cartographic Conference*, 6–10 August 2001, Vol. 5. Beijing, China: LOC of ICC, 3084–3093.

Evenden, G.I., 2005. *libproj4: A comprehensive library of cartographic projection functions (preliminary draft)* [online]. Available from: http://members.verizon.net/~vze2hc4d/proj4/ [Accessed 1 August 2008].

Fenna, D., 2007. *Cartographic science: a compendium of map projections, with derivations*. Boca Raton: CRC/Taylor & Francis.

Garver, J.B., 1988. New perspective on the world. *National Geographic*, 174, 910–913.

Ginzburg, G.A. [[Гинзбург], Г.А.], 1949. Psevdotsilindricheskaya proyektsiya TsNIIGAiK [The pseudocylindrical projection TsNIIGAiK]. *Sbornik Nauchno-Tekhnicheskikh i Proizvodstvennikh Statey GUGK*, 24, 68–72.

Jenny, B. and Patterson, T., 2007. *Flex Projector* [online]. Available from: http://www.flexprojector.com [Accessed 1 August 2008].

Jenny, B., Patterson, T., and Hurni, L., 2008. Flex Projector – interactive software for designing world map projections. *Cartographic Perspectives*, 59, 12–27.

Laskowski, P., 1991. On a mixed local-global error measure for a minimum distortion projection. *ACSM Technical Papers*, 2, 181–186.

Maling, D.H., 1960. A review of some Russian map projections. *Empire Survey Review*, 15, 203–215, 255–266, 294–303.

Ratner, D.A., 1991. An implementation of the Robinson map projection based on cubic splines. *Cartography and Geographic Information Systems*, 18, 104–108.

Richardson, R.T., 1989. Area deformation on the Robinson projection. *The American Cartographer*, 16, 294–296.

Robinson, A., 1974. A new map projection: its development and characteristics. *In*: G.M. Kirschbaum and K.-H. Meine, eds. *International yearbook of cartography*. Bonn-Bad Godesberg, Germany: Kirschbaum, 145–155.

Slocum, T.A., *et al.*, 2009. *Thematic cartography and geovisualization*. Upper Saddle River, NJ: Pearson Prentice Hall.

Snyder, J.P., 1985. Computer-assisted map projection research. *US Geological Survey Bulletin*, 1629, 157.

Snyder, J.P., 1987. *Map projections: a working manual*. Washington, DC: US Geological Survey.

Snyder, J.P., 1990. The Robinson projection: a computation algorithm. *Cartography and Geographic Information Systems*, 17, 301–305.

Snyder, J.P., 1993. *Flattening the earth. Two thousand years of map projections*. Chicago & London: University of Chicago Press.

Tobler, W.R., 1973. The hyperelliptical and other new pseudo cylindrical equal area map projections. *Journal of Geophysical Research*, 78, 1753–1759.

Tobler, W.R., 1977. Numerical approaches to map projections. *In*: I. Kretschmer, ed. *Studies in theoretical cartography*. Vienna: Denticke, 51–64.